An Electron Spin Resonance Study of the Molecular Oxygen Adducts formed by the Cobalt(II) Chelate of Salicylaldazine and Related Systems

By **Thomas D. Smith,* Ivan M. Ruzic,** and **Selwyn Tirant,** Chemistry Department, Monash University, Clayton, Victoria, Australia 3168
John R. Pilbrow, Physics Department, Monash University, Clayton, Victoria, Australia 3168

Cobalt(II) chelates, as well as those of copper(II), nickel(II), and manganese(II), of salicylaldazine, 5,5′-dichlorosalicylaldazine, 3,3′-dimethoxysalicylaldazine, and salicylaldehyde hydrazone have been prepared and characterized by elemental analysis, thermogravimetric analysis, and magnetic susceptibility measurements. The high-spin cobalt(II) chelates form reversible adducts with molecular oxygen in chloroform solutions containing various bases at room temperature. The e.s.r. spectra of the molecular oxygen adducts have been recorded using frozen solutions, and magnetic and structural parameters have been obtained by computer simulation of these spectra. The effect of substituent groups on the ligands and of the various bases present on the numerical values of the parameters is discussed. The electronic mechanisms which contribute to the hyperfine structure observed in the e.s.r. spectra of the molecular oxygen adducts have been reassessed. Within the terms of the model, indirect spin-polarization effects appear to be overshadowed by direct effects in many cases.

THE effects of various substituents and structural variations of the ligand *NN*′-ethylenebis(salicylideneimine) (H_2salen) on the e.s.r. spectra and magnetic parameters of the molecular oxygen adducts formed by cobalt(II) chelates in the presence of nitrogenous bases were described earlier.[1] The structure of salicylaldazine, formed by the condensation of salicylaldehyde with hydrazine,[2] is similar to that of salen, the difference lying in the absence of the bridging CH_2CH_2 group in salicylaldazine. The preparation of a number of transition-metal compounds of salicylaldazine has been reported,[3] while the i.r. spectra of the ligand [4] and related systems have been discussed.[5,6] Salicylaldehyde hydrazone, formed by condensation of salicylaldehyde and hydrazine in 1 : 1 mole ratio, also forms chelates with a range of metal ions [7–9] and provides a further structural variation for the study of the molecular oxygen adduct of its cobalt(II) chelate.

RESULTS

The elemental analysis, magnetic susceptibility measurements, i.r. spectral, and thermogravimetric data indicate that the cobalt(II) chelates of salicylaldazine, 5,5′-dichlorosalicylaldazine, and 3,3′-dimethoxysalicylaldazine exist as dihydrated high-spin compounds. Identical conclusions are reached concerning the formation of the copper(II), nickel(II), and manganese(II) compounds.

On passing molecular oxygen through a chloroform solution of cobalt(II) salicylaldazinate containing pyridine (20% v/v), prepared under nitrogen, the reddish brown colour of the solution acquires a darker hue as shown in Figure 1. The oxygenation process is reversible, since, when dry nitrogen is passed through the solution for *ca.* 5 min, the solution returns to its original colour. This process may be repeated through several cycles.

A sample of the chloroform solution of cobalt(II) salicylaldazinate (salaz) containing pyridine (20% v/v), prepared under nitrogen, does not possess an e.s.r. spectrum at 140 K. On the other hand, when treated with dry molecular oxygen the solution gives rise to an e.s.r. spectrum typical of that observed for the molecular oxygen adducts of cobalt(II) compounds as outlined in Figure 2. A number of studies have shown that the addition of base has a marked effect on the degree of oxygenation of cobalt(II) chelates and also on the magnetic parameters associated with the characteristic e.s.r. signals due to the molecular oxygen adducts of cobalt(II) chelates. A striking example of this was found in a study of the addition of various bases to cobalt(II) tetra(*p*-tolyl)porphyrinato-complexes.[10] Addition of 1,3,5-trinitrobenzene, picric acid, pyrene, acridine, 2,4-dimethylpyridine, and 2,4,6-trimethylpyridine to toluene solutions of the cobalt(II) porphyrin brings about a wide variation in the e.s.r. spectra of the molecular oxygen adducts. In the present investigation, the e.s.r. spectra of the molecular oxygen adducts of cobalt(II) salicylaldazinate formed in chloroform in the presence of a similar range of bases which include acridine, 2-methylpyridine, 2,4,6-trimethylpyri-

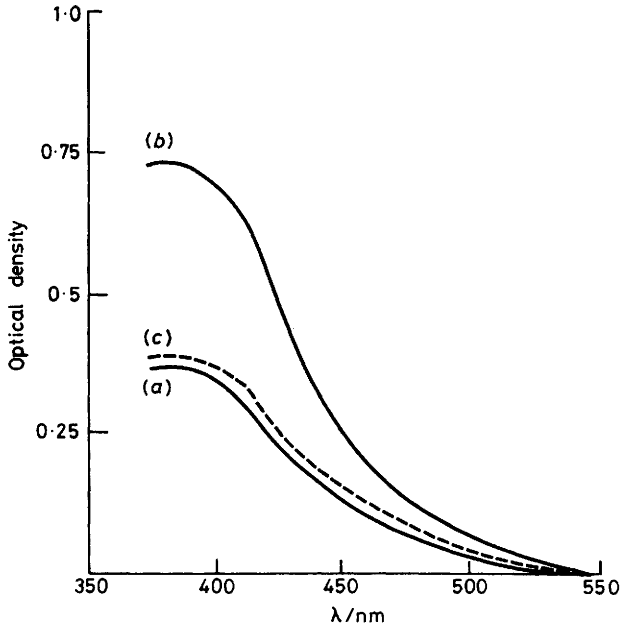

FIGURE 1 U.v.–visible absorption spectra of the cobalt(II) salicylaldazinate chelate under nitrogen and oxygen atmospheres in chloroform containing pyridine (10% v/v) (path-length 1 cm). (*a*) Under nitrogen, (*b*) + oxygen, (*c*) + nitrogen

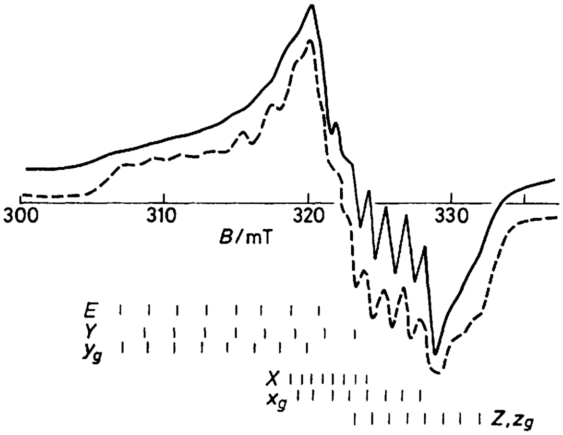

FIGURE 2 E.s.r. spectrum due to the molecular oxygen adduct of cobalt(II) salicylaldazinate in chloroform containing pyridine (10% v/v) at 100 K. The dashed line shows the computer simulation using the parameters listed in Table 3. The stick spectra labelled *E*, correspond to extremum lines (arising from a non-principal direction) and *X*, x_g, *Y*, y_g, and *Z*, z_g to principal axes directions respectively

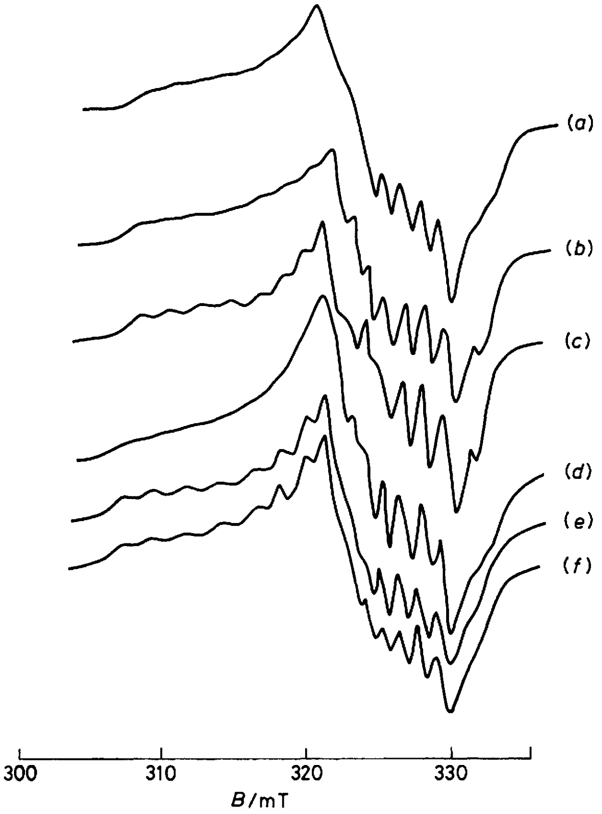

FIGURE 3 E.s.r. spectra due to the molecular oxygen adduct of cobalt(II) salicylaldazinate in chloroform containing 10% v/v of (*a*) 2,4,6-trimethylpyridine, (*b*) 2,4-dimethylpyridine, (*c*) acridine, (*d*) pyridine, (*e*) 2-methylpyridine, and (*f*) 2,6-dimethylpyridine (see Table 3)

dine, 2,4-dimethylpyridine, and 2,6-dimethylpyridine have been studied, the results being shown in Figure 3.

The e.s.r. spectrum due to the molecular oxygen adduct of cobalt(II) salicylaldazinate was also studied in dimethylformamide and dimethyl sulphoxide. In addition, the presence of substituent groups 3-methoxy- and 5-chloro- on the phenyl groups of the ligand produced a discernible effect on the e.s.r. spectrum of the molecular oxygen adduct of the cobalt(II) chelate.

The elemental analysis, magnetic susceptibility, and thermogravimetric properties of the cobalt(II) chelate of salicylaldehyde hydrazone, as in the case of the copper(II), nickel(II), manganese(II), and iron(II) chelates, show that it exists in the high-spin form $[Co^{II}(salhy)_2]\cdot 2H_2O$ where salhy$^-$ is the anionic form of salicylaldehyde hydrazone. The formation of molecular oxygen adducts of the cobalt(II) chelate occurs reversibly at room temperature in chloroform solutions containing pyridine. The e.s.r. spectrum of the adduct in frozen solution was observed and compared to that due to other solutions of the chelate containing various nitrogen bases. Little variation of the e.s.r. spectra could be discerned. However, the presence of 3-methoxy- or 5-chloro- substituent groups on the phenyl ring of the ligand anion produces a marked effect on the e.s.r. spectrum of the molecular oxygen adduct of the cobalt(II) chelate.

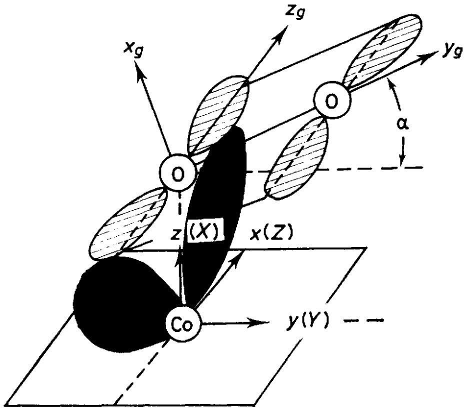

FIGURE 4 Arrangement of *g* and *A* principal axes for $Co^{II}(O_2)$ adduct with assumed C_s molecular symmetry; *x*, *y*, *z* used to conform to nomenclature of ref. 16; $A_x = A_Z$, $A_y = A_Y$, $A_z = A_X$. The planar part of the parent complex is outlined but more evidence would be needed to establish the orientation unequivocally in each case. The unpaired electron π^* orbital (hatched) and the relevant part of the cobalt d_{xz} orbital (filled in) are depicted schematically to illustrate the point that, as α increases, π^*–d_{xz} overlap should increase and possibly go through a maximum at α_m

A satisfactory molecular model of cobalt oxygen adducts was outlined previously.[1,11] It is depicted in Figure 4, showing C_s local symmetry, and takes into account the spatial disposition of the oxygen molecule with respect to the cobalt atom, as well as the symmetry properties of the *g* and *A* tensors. A spin Hamiltonian appropriate to this model is shown in equation (1) where *S* is the effective

$$\mathscr{H} = \beta \sum_{i = x_g, y_g, z_g} g_i B_i S_i + \sum_{j = X, Y, Z} A_i S_i I_i \qquad (1)$$

electron spin ($\frac{1}{2}$) and $I = \frac{7}{2}$ for the electron nuclear hyperfine interaction involving cobalt. In this paper x_g, y_g, and z_g are used to denote the *g* principal directions whereas *x*, *y*, and *z* are used for hyperfine co-ordinates on the cobalt atom (Figure 4).

The computer-simulation program previously described by us[12] is based upon the following standard algebraic relationships which hold when the Zeeman interaction is very much larger than the cobalt hyperfine interaction, a condition certainly fulfilled by Co–O_2 adducts. These are as follows: for g-value variation with orientation, where l_x, l_y, and l_z are direction cosines of the magnetic field B with g principal axes, equation (2), and for the hyperfine interaction, where X, Y, Z, and α are all defined in Figures 4 and 5, equation (3), where $x = x_g$ *etc.* in both cases. At a particular orientation of B relative to the molecular axes, the resonance fields are given by equation (4). The second-order variables, a and b, are not written out in full although they are automatically included in the simulation even though their magnitudes will not be very significant for Co–O_2 adducts where the hyperfine constants are in the range *ca.* 7 to *ca.* 20×10^{-4} cm^{-1}. Other corrections allowed for in the simulation procedure are g anisotropy in the transition probability,[13] the $1/g$ field-frequency transformation factor,[14] and linewidth anisotropy. The latter was found to be necessary but the actual values have not been reported here.

$$g^2 = g_x^2 l_x^2 + g_y^2 l_y^2 + g_z^2 l_z^2 \quad (2)$$

$$g^2A^2 = A_X^2(g_x l_x \cos\alpha + g_y l_y \sin\alpha)^2 + A_Y^2(-g_x l_x \sin\alpha + g_y l_y \cos\alpha)^2 + A_Z^2 g_z^2 l_z^2 \quad (3)$$

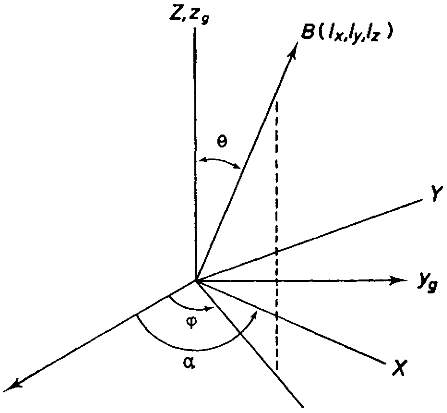

FIGURE 5 Co-ordinate system for monoclinic symmetry. For C_s symmetry, z_g and Z are common g and A axes normal to mirror plane. See also Figure 4. In contrast to Figure 4, all the axes have been drawn from a common origin to assist understanding of the spin Hamiltonian, equation (1)

$$B = B_0 - (A/g\beta)M_I - a[I(I + 1) - M_I^2] - bM_I^2 \quad (4)$$

In view of the fact that not all examples of Co–O_2 e.s.r. spectra have been interpreted according to monoclinic or lower symmetry, we now consider some important factors which are relevant to the analysis of such data. When the Zeeman interaction is much larger than the hyperfine constants, as for Co–O_2 adducts, the turning directions in a crystal must correspond to the principal g directions (x_g, y_g, z_g). In the e.s.r. spectra of powdered samples it is the turning directions, where $\partial B/\partial\theta = 0$ and or $\partial B/\partial\phi = 0$, which produce the sharp features observed. Only when the symmetry is at least as high as orthorhombic ($\alpha = 0$ in Figures 4 and 5) do the observed hyperfine splittings correspond to the principal hyperfine components in every case. When $\alpha \neq 0$, and the complex has C_s symmetry, only A_Z could, in principle, be measured directly from a powder spectrum, although it may be hard to measure because of overlap between 'z' spectra and other contributions. In single crystals where the symmetry is low, hyperfine splittings must maximize or minimize at directions different from the g axes.

An orthorhombic approximation to the Co–O_2 adducts may yield correct peak positions, however it is not possible to match intensities satisfactorily. Furthermore, the hyperfine constants so obtained will not necessarily be correct; at least one of them will be too high, and another too low. In the former case where $\alpha \neq 0$, one must integrate over ϕ in the range 0–180° whereas, when $\alpha = 0$, ϕ ranges only from 0 to 90°. Figure 6 illustrates the effect of changing α while keeping all other parameters the same.

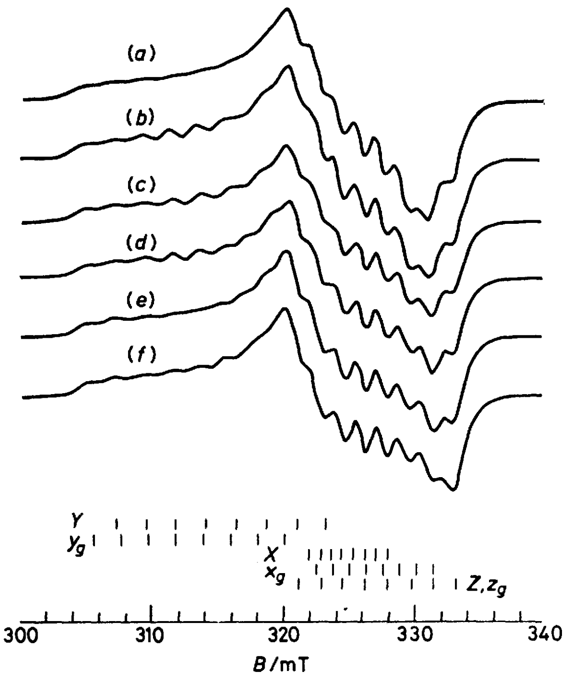

FIGURE 6 Simulated e.s.r. spectra for Co^{II}(O_2) adduct illustrating effect of variation in α: $\alpha = 0$ (*a*), 5 (*b*), 10 (*c*), 15 (*d*), 20 (*e*), and 25° (*f*); g and A values as for [Co^{II}(tpps)(O_2)] (tpps = 5,10,15,20-tetra-*p*-sulphophenylporphyrinate) (ref. 11, Table 2). Linewidths used are $\sigma_x = \sigma_y = 1.2$ mT and $\sigma_z = 1.0$ mT. Microwave frequency 9 143 MHz. (See Figures 4 and 5 for relation between axes and molecular axes)

To illustrate the importance of chosing a realistic symmetry model for Co–O_2 adducts, the spectra reported by Niswander and Taylor[15] for a series of cobalt(II) Schiff-base molecular oxygen adducts have been reviewed. Niswander and Taylor interpreted their results using orthorhombic symmetry. Their spectra have been digitized and the resulting spectra simulated using the model described in Figure 4. It was necessary to relabel the axes to conform to our simulation program. The results are given in Table 1 along with the results of Taylor and Niswander which are given in parentheses. In Table 1 we also include calculations of the hyperfine splittings along the principal g directions, x_g and y_g axes, respectively. These are as given in equations (5a) and (5b), from equation (3).

$$A(x_g)^2 = A_X^2 \cos^2\alpha + A_Y^2 \sin^2\alpha \quad (5a)$$

$$A(y_g)^2 = A_X^2 \sin^2\alpha + A_Y^2 \cos^2\alpha \quad (5b)$$

The results in Table 1 make it quite clear that one cannot be sure that hyperfine values measured from a spectral chart are true principal values. As a consequence of the reinterpretation of the data, g values show the most marked difference for the intermediate value (g_x) which is not surprising for it is usually the most difficult one to determine

TABLE 1

E.s.r. parameters[a] for some Co–O_2 adducts

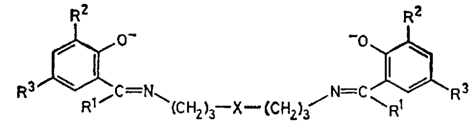

L

Complex	L: X	R1	R2	R3	α/°	$A_z(X)$[b] (10-4cm-1)	$A_y(Y)$[b]	$A_x(Z)$[b]	⟨A⟩	$A(x_g)$	$A(y_g)$	g_x[c]	g_y[c]	g_z[c]	Ref.[d]
(1)	NH	H	H	H	26 (0)	5.7	24	9.9 (13.5)	13.2	11.7 (13.3)	21.7 (22.7)	2.016 (2.007)	2.084 (2.085)	1.996 (2.000)	Figure 4(*a*)
(2)	NCH_3	H	OCH_3	H	28 (0)	6.5	20.0	10.0 (14.5)	12.2	11.0 (12.1)	17.9 (18.6)	2.014 (2.009)	2.090 (2.090)	1.995 (1.988)	Figure 4(*b*)
(3)	NCH_3	CH_3	H	H	28 (0)	6.3	22.4	11.0 (14.9)	13.2	11.8 (13.0)	21.2 (19.7)	2.009 (2.004)	2.088 (2.089)	1.993 (1.998)	Figure 5(*a*)
(4)	NPh	H	H	H	27 (0)	8.2	24.8	12.2 (17.0)	15.1	13.4 (16.0)	22.4 (22.6)	2.012 (2.004)	2.088 (2.080)	1.990 (1.997)	Figure 5(*b*)
(5)	O	H	H	Cl	27—28 (0)	7.5	31.3	15.0 (19.1)	17.9	15.7 (16.4)	28.1 (27.6)	2.013 (2.003)	2.089 (2.090)	1.988 (1.995)	Figure 6(*a*)
(6)	PCH_3	H	OCH_3	H	29 (0)	6.4	27.0	12.3 (19.1)	15.2	14.2 (14.3)	23.8 (23.6)	2.014 (2.009)	2.086 (2.097)	1.987 (2.000)	Figure 6(*b*)

[a] For definitions of axes see Figure 4. [b] Errors in *A* values $\pm 0.5 \times 10^{-4}$ cm^{-1}; assumed negative for hyperfine analysis. [c] Errors in *g* values $< \pm 0.001$. [d] Based on ref. 15. (Published spectra were digitized and simulated at Monash University by I. Ruzic. Axes relabelled to conform to monoclinic simulation program. *g* and *A* values in parentheses are those reported by Niswander and Taylor. α value in parentheses is that implied by the orthorhombic model of these authors.)

from a powder spectrum. (Errors quoted in Tables 1—5 for *g* and *A* values and α are based on goodness-of-fit criteria judged by eye. Automatic least-squares fitting methods have not been used because of computer time limitations.)

DISCUSSION

In the present work the precursor cobalt(II) compounds, the cobalt(II) chelates of salicylaldazine, reversibly form molecular oxygen adducts at room temperature in the presence of nitrogenous bases. Their e.s.r. spectra observed in frozen solutions enable substituent effects to be studied as well as the influence of the bases on the spatial disposition of the molecular oxygen with respect to the cobalt centre. As shown by Table 2, the angle α is a little higher in the cobalt(II) salicylaldazinate–molecular oxygen adduct compared with that observed previously in the molecular adduct of *NN'*-ethylenebis(salicylideneiminato)cobalt(II), [Co^{II}(salen)].[1] Substitution of the methoxy-group into the phenyl ring of salicylaldazine or salicylaldehyde hydrazone leads to a diminution in the value of α and an increase in the magnitude of A_X as observed previously for the quadridentate Schiff-base chelates.[1] Table 3 shows that larger effects on the magnetic parameters occur as a result of changes of the base associated with the cobalt(II) salicylaldazinate–molecular oxygen adduct. For the purpose of comparisons, taking pyridine as the starting point, the presence of 2,4,6-trimethylpyridine causes a marked drop in the value of α and an increase in the value of A_X, whereas the presence of 2,6-dimethylpyridine favours an increase in the value of α and a decrease in the value of A_X. The structural effects and changes to the hyperfine term A_X brought about by the bases are interesting to compare, since both bases possess the same degree of steric hindrance but differ in the substituent present at the 4-position. Again comparing the structural and hyperfine effects which accrue from taking the bases 2,4-dimethylpyridine and 2-methylpyridine, both of which have similar steric requirements at the nitrogen, but differ in the substituent in the 4-position, the former favours a lower value of α while the latter gives a higher value of α. A reasonable conclusion from these limited comparisons is that the controlling factor is the presence of a methyl group in the 4-position. Electron-density transfer from the methyl

TABLE 2

Magnetic parameters associated with the molecular oxygen adducts of cobalt(II) chelates of salicylaldazinate (salaz), 3,3'-dimethoxysalicylaldazinate (dmsalaz), and 5,5'-dichlorosalicylaldazinate (dcsalaz) in chloroform containing pyridine (20% v/v) *

Compound	g_x	g_y	g_z	$10^4A_z(X)$ (cm^{-1})	$10^4A_y(Y)$ (cm^{-1})	$10^4A_x(Z)$ (cm^{-1})	α/°
[Co(dmsalaz)(O_2)]	2.010	2.081	1.994	10.3	20.2	7.6	27
[Co(salaz)(O_2)]	2.016	2.082	1.991	7.2	20.3	11.6	29
[Co(dcsalaz)(O_2)]	2.010	2.081	1.994	7.3	19.0	7.0	30

* Errors as in Table 1.

TABLE 3

Magnetic parameters associated with the molecular oxygen adducts of the cobalt(II) salicylaldazinate chelate in chloroform containing various bases (20% v/v) at 77 K (ν = 9 149 MHz)

Base	g_x	g_y	g_z	$10^4A_z(X)$ (cm^{-1})	$10^4A_y(Y)$ (cm^{-1})	$10^4A_x(Z)$ (cm^{-1})	α°
2,4,6-Trimethylpyridine	2.017 ± 0.005	2.081 ± 0.002	1.995 ± 0.002	10.5 ± 0.05	17.5 ± 1	11.6 ± 0.5	22 ± 1
2,4-Dimethylpyridine	2.018	2.082	1.993	5.0	20.5	8.8	27
Acridine	2.012	2.083	1.995	5.8	20.2	10.5	27
Pyridine	2.016	2.082	1.991	7.2	20.3	11.6	29
Methylpyridine	2.015	2.081	1.994	5.8	20.5	10.6	30
2,6-Dimethylpyridine	2.017	2.081	1.993	5.0	20.5	8.8	32
Dimethylformamide	2.011	2.081	1.994	7.0	20.5	10.0	28

group to the nitrogen is able to offset the effect of steric hindrance caused by the methyl groups in the 2- or 2,6-positions.

Table 4 shows that the presence of the methyl group in the 4-position of the base co-ordinated to the molecular oxygen adduct of the chelate [*o*-phenylenebis(salicylideneiminato)]cobalt(II), [Co^{II}(salphen)], again leads to a diminution in the value of α and an increase in the value of A_X.

TABLE 4

Magnetic parameters associated with the molecular oxygen adducts of cobalt(II) chelates of the 3-methoxysalicylaldehyde hydrazone (msalhy) and 5-chlorosalicylaldehyde (csalhy) hydrazone anions in chloroform containing pyridine (20% v/v) at 77 K *

Compound	g_x	g_y	g_z	$10^4 A_z(X)$	$10^4 A_y(Y)$	$10^4 A_x(Z)$	α/°
					cm^{-1}		
[Co(msalhy)$_2$(O$_2$)]	2.017	2.081	1.995	8.3	18.5	10.0	18
[Co(salhy)$_2$(O$_2$)]	2.019	2.091	1.998	6.2	18.5	9.6	21
[Co(csalhy)$_2$(O$_2$)]	2.019	2.088	1.999	10.3	17.4	10.5	25

* Errors as in Table 1.

E.S.R. Parameters due to Cobalt(II)*–Dioxygen Adducts.*—Models invoked to account for the electronic properties of cobalt(II) chelate–molecular oxygen adducts and their e.s.r. paramaters are of two main types. A frequently discussed picture consists of an O_2^- radical thought to result from almost complete electron transfer from cobalt(II) to molecular oxygen. On the other hand, the work of Drago and co-workers[16-18] and also Dickinson and Chien[19] recognizes the importance of indirect spin-polarization contributions to hyperfine structure and the formation of a Co–O$_2$ bond with electron transfer occurring in the bonding region. Our conclusion (see later) is that both direct and indirect hyperfine couplings are required to account for the observed cobalt hyperfine structure.

Superoxide formulation. Within the superoxide formulation, cobalt hyperfine structure is understood as arising from partial occupation of one or more *d* orbitals by the unpaired electron on the oxygen. If the cobalt hyperfine splittings (h.f.s.) were due solely to admixture of d_{xz} with the maximum h.f. constant along *y* (Figure 4), then, as pointed out many years ago by Hoffman *et al.*,[20] equations (6a)—(6c) hold where g_n and β_n are the nuclear

$$A_x = A_z \approx P(-K + \tfrac{2}{7}\gamma^2) \qquad (6a)$$

$$A_{\text{max.}} = A_y \approx P(-K - \tfrac{4}{7}\gamma^2) \qquad (6b)$$

$$P = 2\beta g_n \beta_n \langle r^{-3} \rangle_{\text{Co}} \qquad (6c)$$

g factor and nuclear magneton respectively. Here, we use τ for the mixing coefficient (Hoffman *et al.* used α) to avoid confusion with the non-coincidence angle α (Figures 4 and 5). Rearranging the equations one obtains equations (7) and (8).

$$|A_{\text{max.}}| \simeq |\langle A \rangle| + \tfrac{4}{7}P\tau^2 \qquad (7)$$

$$\langle A \rangle = \tfrac{1}{3}(A_X + A_Y + A_Z) \qquad (8)$$

Typically, analysis of cobalt h.f.s. due to Co–O$_2$ adducts yields $\tau^2 \approx 0.1$, a value which would indicate more or less complete electron transfer from cobalt to oxygen. Tovrog *et al.*[16] have pointed out that attempts to determine a value for τ^2 from 4*s*-electron admixtures yield a value of *ca.* 0.5. It is as a result of such a discrepancy that explanations based upon spin-pairing models have been sought.

Equations similar to (6a) and (6b) have been used in connection with d_{z^2} rather than d_{xz} admixture but the former puts $A_{\text{max.}}$ along *z*.

Spin-pairing model. Dickinson and Chien[19] found that the anisotropic cobalt h.f.s. for cobalt–myoglobin–dioxygen was due to positive spin density on d_{xz} (their d_{yz}) and negative spin density on d_{yz} (their d_{xz}). In a review of ^{17}O hyperfine splittings observed for [Co(bzacacen)(O$_2$)] [bzacacen = *NN'*-ethylenebis(benzoylacetoneiminate)] Tovrog *et al.*[16] concluded that the total oxygen spin density was 1 with 0.4 on the middle oxygen, nearest cobalt, and 0.6 on the outer oxygen. They concluded that the observed cobalt h.f.s. must be largely due to an indirect effect and postulated a spin-polarization mechanism in which spin was not directly transferred to cobalt *d* orbitals. The foregoing conclusions are based upon the assumption that *all* the hyperfine constants are negative, a conclusion which could only be confirmed by use of ENDOR. What is known is that all the signs must be the same.

Spin-pairing concepts are by no means new and in similar or related contexts have been mentioned by Wayland *et al.*[21] and, from a Heitler–London point of view, by Harcourt,[22] the simpler models requiring consideration of three electrons. Support for these ideas may be found in results of molecular-orbital calculations.[23,24]

Before going into details of the spin-polarization model put forward by Tovrog *et al.*,[16] but which must be modified as will be explained, two observations are necessary. The observed h.f. constants must first be corrected for the direct electron (oxygen)–nuclear (cobalt) dipole–dipole interaction. Tovrog *et al.*[16] used the co-ordinates for [Co(bzacacen)(O$_2$)] reported by Rodley and Robinson.[25] A tilt to the dipolar axes caused by the fact that the cobalt–terminal oxygen direction is *not* along *z* was neglected because it is a small effect. The resultant value for both oxygens is given by equation (9) resulting

$$A_{\text{dip}} = (\overset{x}{-0.5}, \overset{y}{-0.5}, \overset{z}{1.0}) \times 10^{-4}\ \text{cm}^{-1} \qquad (9)$$

from the use of the equations (10a) and (10b).

$$A_{\text{dip}}(x,y) = -\, g\beta g_n \beta_n / r^3 \qquad (10a)$$

$$A_{\text{dip}}(z) = 2 g\beta g_n \beta_n / r^3 \qquad (10b)$$

Tovrog *et al.*[16] found that there were difficulties in connection with the extent of the *s*-electron contribution from cobalt 4*s* and so concentrated upon the *d*-electron or anisotropic part of the hyperfine structure. They then sought to explain the observations by invoking spin polarization of d_{z^2}. This does not adequately account for the e.s.r. results, since it puts $A_{\text{max.}}$ along *z* whereas there is good evidence that it should be along *y*.

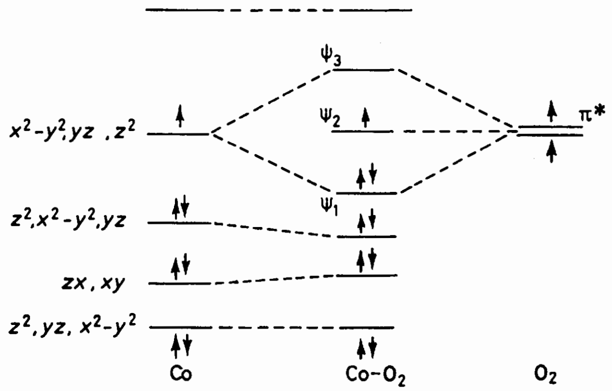

FIGURE 7 Simplified molecular-orbital scheme for $Co^{II}(O_2)$ adducts with C_s symmetry, adapted from ref. 16. Not all possible interactions are illustrated, *e.g.* the direct overlap of d_{xz} and ψ_2 is not shown

The general idea for spin pairing is shown in Figure 7 where to sum up the various contributions by Tovrog *et al.*[16] and Dickinson and Chien [19] the Tovrog *et al.* model is modified as follows: ψ_1 should include d_{yz} as well as d_{z^2}, therefore we write equation (11) while the unpaired

$$\psi_1 = \alpha'\, d_{z^2} + \alpha'''\, d_{yz} + \gamma(4s) + \beta\pi^*(x_g) \qquad (11)$$

electron, originally in a π^* orbital on the oxygen molecule, is, according to the back-bonding argument of Tovrog *et al.*, described by equation (12). As far as is possible, the notation agrees with that used by Tovrog *et al.* The

$$\psi_2 = e\pi^*(z_g) + \alpha''\, d_{xz} \qquad (12)$$

orbital ψ_3 is unfilled. Since d_{z^2} and d_{yz} transform according to the same representation of C_s (putting *x* normal to the mirror plane) then their individual contributions to the spin-polarization mechanism cannot be separated. In Figure 7, the *d* orbitals are labelled according to C_s symmetry and not according to the nearly tetragonal symmetry appropriate to many of the parent chelates.

In order to separate the various contributions to the cobalt h.f.s. the following equations [(13a)—(13c)] should be considered where *f* and *h*, assumed to arise from

$$A_x - \langle A\rangle = a_x = \tfrac{2}{7}(f + g + 2h) \qquad (13a)$$

$$A_y - \langle A\rangle = a_y = \tfrac{2}{7}(f - 2g + h) \qquad (13b)$$

$$A_z - \langle A\rangle = a_z = \tfrac{2}{7}(-\,2f + g - h) \qquad (13c)$$

indirect spin polarization of d_{z^2} and d_{yz} respectively by the unpaired electron, especially that on the middle oxygen of spin density ρ_O, are given by equations (14a) and (14b); $U_{Co\text{-}O}$ is a spin-polarization constant. For

$$f = P\rho_O U_{Co\text{-}O}\alpha'^2 \qquad (14a)$$

$$h = P\rho_O U_{Co\text{-}O}\alpha'''^2 \qquad (14b)$$

the ***direct*** h.f. contribution from d_{yz}, equation (14c) holds.

$$g = P\alpha''^2 \qquad (14c)$$

The use of *g* is not to be confused with the *g* values referred to earlier but is retained here to be consistent with the notation of Tovrog *et al.* Tables 6—10 give the results of the foregoing analysis for the data reported in

TABLE 5

Magnetic parameters associated with the molecular oxygen adducts of cobalt(II) chelates of $[Co^{II}(salphen)]$ in chloroform containing various nitrogenous bases (20% v/v) *

Base	g_x	g_y	g_z	$10^4A_z(X)$	$10^4A_y(Y)$ cm⁻¹	$10^4A_x(Z)$	α/°
2,4-Dimethylpyridine	2.020	2.093	1.991	8.3	22.5	10.0	27
Pyridine	2.023	2.081	1.994	7.0	20.5	10.0	30
2-Methylpyridine	2.011	2.081	1.994	7.0	20.5	10.0	31

* Errors as in Table 1.

TABLE 6

Cobalt hyperfine analysis: cobalt Schiff-base–O_2 adducts

Compound [a]	10^4a_x	10^4a_y cm⁻¹	10^4a_z	$f + h$	$g + h$	Ref.
(1)	3.8	−10.3	6.5	−3.2	16.5	*b*
(2)	2.7	−7.3	−4.7	−2.7	12.0	*b*
(3)	2.7	−8.7	5.9	−4.3	13.3	*b*
(4)	3.4	−9.3	5.9	−2.9	11.8	*b*
(5)	3.4	−12.9	9.4	−7.0	19.0	*b*
(6)	3.4	−11.3	7.8	−5.1	17.2	*b*
$[Co(salen)(O_2)]$ (also salpd, salpn)	4.3	−7.2	3.0	1.5	13.4	*c*
$[Co(\alpha Me\text{-}salen)(O_2)]$ (also αEt-salen)	3.0	−7.5	4.5	−1.8	12.3	*c*
[Co(3OMe-salen)] (also salen)	5.6	−6.4	0.7	5.7	14.0	*c*

[a] See Table 1 for formulae of complexes (1)—(6). Ligand abbreviations: salpd = *NN'*-propane-1,3-diylbis(salicylideneiminate); salpn = *NN'*-propane-1,2-diylbis(salicylideneiminate). [b] Data based on recalculated values outlined by Table 1. [c] Data based on ref. 1.

Tables 1—5. Equations (13) have been rearranged to give equations (15a) and (15b).

$$a_x - a_z = \tfrac{6}{7}(f + h) \qquad (15a)$$

$$a_x - a_y = \tfrac{6}{7}(g + h) \qquad (15b)$$

It is unfortunate that individual values of *f*, *g*, and *h* cannot be obtained. Some general observations will have to suffice. For the Schiff-base data (Table 6) and the base variation (Table 7), $(g + h)$ values lie mainly in the range 10—17. Suppose for the moment that $h \approx 0$, then the limiting values of *g* imply that $\alpha''^2 \leqslant 0.06$, consistent with the requirement laid down by Tovrog *et al.*[16] that back bonding be small. In obtaining the estimate of α''^2 it was assumed that $P \approx 0.02$ cm^{-1}. Within the terms of reference of the model, almost all of the values of $(f + h)$ are negative, implying either that the hyperfine contributions from d_{z^2} and d_{yz} are direct, arising from a positive spin density, or that the model is inadequate. Indeed, for C_s symmetry, putting *x* normal to the mirror plane, then ψ_1 should be augmented by $d_{x^2-y^2}$ and ψ_2 by d_{xy}. Such additions would introduce two more parameters into the problem but these cannot, at present, be handled. Nevertheless, there are two good cases illustrated by Tables 7 and 9 in which there is a trend from indirect coupling (positive values of $f + h$) to direct coupling (negative values of $f + h$) involving d_{z^2} and d_{yz} cobalt orbitals.

TABLE 7

Cobalt hyperfine analysis: substituent effects based on e.s.r. data in Table 2

Compound *	10^4a_x	10^4a_y cm^{-1}	10^4a_z	$f + h$	$g + h$
[Co(dmsalaz)(O$_2$)]	5.6	−7.0	1.4	6.0	15.8
[Co(dcsalaz)(O$_2$)]	4.5	−6.5	3.0	1.8	12.9
[Co(salaz)(O$_2$)]	1.9	−6.8	4.8	−3.3	10.2

* dmsalaz = 3,3′-Dimethoxysalicylaldazinate, dcsalaz = 5,5′-dichlorosalicylaldazinate.

TABLE 8

Cobalt hyperfine analysis: base variation in cobalt(II) salicylaldazinate–O$_2$ (based on e.s.r. data in Table 3)

Base	10^4a_x	10^4a_y cm^{-1}	10^4a_z	$f + h$	$g + h$
2,4,6-Trimethylpyridine	2.1	−4.2	1.7	0.5	7.4
2,4-Dimethylpyridine *	3.1	−8.6	5.4	−2.7	13.7
Acridine	2.2	−7.5	5.4	−3.7	11.3
Pyridine	1.9	−6.8	5.2	−3.8	10.2
2-Methylpyridine	2.2	−7.7	5.5	−3.8	11.6
2,6-Dimethylpyridine *	3.1	−8.6	5.4	−2.7	13.7
Dimethylformamide	3.0	−7.5	4.5	−1.8	12.3

* *g* Values differ slightly. Within fitting errors *A* values identical.

An attempt to correlate the various parameters deduced from the hyperfine analysis is shown in Figure 8. In Figure 8(*a*) the $(f + h)$ *versus* $(g + h)$ correlation shows two kinds of behaviour. The bulk of the results have negative $(f + h)$ values, implying net direct hyperfine coupling involving d_{yz} and d_{z^2} orbitals, and they lie within a region bounded by the dashed lines. These results suggest that the greater the overlap of the unpaired electron π^* orbital on oxygen with d_{xz}, the greater it is also with d_{yz} and d_{z^2}. The points represented by open circles come from a study of substituent effects for some Schiff-base adducts[1] showing that the greater the change near the cobalt(II) produced by the methoxy-substituent, the larger is the observed indirect effect. The open squares represent substituent effects for salicylaldazine complexes, where again the methoxy-substitution gives a large net indirect hyperfine coupling involving d_{yz} and d_{z^2}. Correlations of $(f + h)$ *versus* α and $(g + h)$ *versus* α are given by Figures 8(*b*) and 8(*c*) respectively. While in Figure 8(*b*) the substituent-effect results stand separately from the remainder, and although they are correlated linearly within each group in Figure 8(*c*), all the points in that case are found to lie within the same family of results. The broad conclusion which is tentatively suggested is that, as α increases, $(f + h)$ becomes more negative, suggesting increased overlap of π^* and (d_{yz}, d_{z^2}). From Figure 8(*c*), there is the faintest suggestion of a maximum in $(g + h)$ at α *ca.* 26° which may be understood by reference to Figure 4 where an increase in α should lead to an increase in π^*–d_{yz} overlap, an overlap which might conceivably go through a maximum.

TABLE 9

Cobalt hyperfine analysis (based on e.s.r. data in Table 4)

Compound *	10^4a_x	10^4a_y cm^{-1}	10^4a_z	$f + h$	$g + h$
[Co(csalhy)$_2$(O$_2$)]	2.7	−4.2	1.4	1.2	8.4
[Co(msalhy)$_2$(O$_2$)]	2.8	−5.7	3.0	−0.2	9.9
[Co(salhy)$_2$(O$_2$)]	2.3	−6.6	4.2	−2.2	10.4

* csalhy = 5-Chlorosalicylaldehyde hydrazone anion; msalhy = 3-methoxysalicylaldehyde hydrazone anion.

TABLE 10

Cobalt hyperfine analysis: base variation in [Co$^{\text{II}}$(salphen)] in chloroform (based on e.s.r. data in Table 5)

Base	10^4a_x	10^4a_y cm^{-1}	10^4a_z	$f + h$	$g + h$
2,4-Dimethylpyridine	4.1	−8.4	4.3	−0.2	14.6
Pyridine	3.0	−7.5	4.5	−1.8	12.3
2-Methylpyridine	3.0	−7.5	4.5	−1.8	12.3

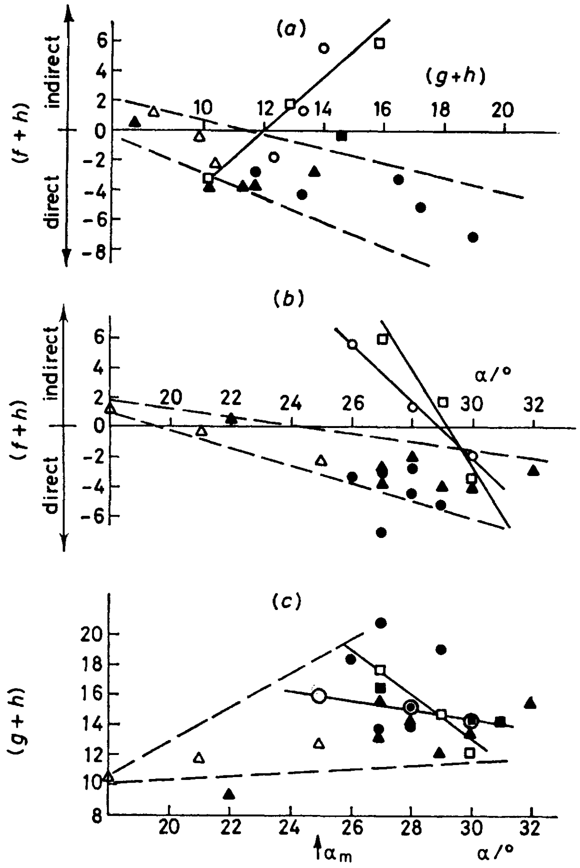

FIGURE 8 Correlation diagrams for cobalt hyperfine parameters for cobalt–oxygen adducts: (*a*) $(f + h)$ *versus* $(g + h)$; (*b*) $(f + h)$ *versus* α; and (*c*) $(g + h)$ *versus* α. (●), Cobalt Schiff-base adducts, reinterpreted results based on ref. 15 (Tables 1 and 6); (○), cobalt Schiff-base adducts, substituent effects[1] (Table 6); (□), cobalt salicylaldazine–oxygen adducts in chloroform–pyridine solution (Tables 2 and 7); (▲), cobalt salicylaldazine–oxygen adducts, base variation (Tables 3 and 8); (△), cobalt salicylaldehyde hydrazone–oxygen adducts, substituent effects (Tables 4 and 9); (■), [Co(salphen)]–oxygen adducts, base variation (Tables 5 and 10). Error bars are not shown but the values of $(f + h)$ and $(g + h)$ probably have errors of ±1. Errors in α lie most probably in the range ±1 to ±2°. In some cases the error in α could be higher

In the small number of cases where $(f + h) > 0$, one might hope to compare Co^{II}–O_2 e.s.r. spectra with those of a comparable NO adduct, a method used by Tovrog *et al.*[16] Using subscripts O and N to distinguish O_2 and NO adducts, equations (16a) and (16b) might be compared. The nitroxide data used by Tovrog *et al.*[16]

$$f_O + h_O = P\rho_O U_{Co\text{-}O}(\alpha_O'^2 + \alpha_O'''^2) \qquad (16a)$$

$$f_N + h_N = P\rho_N U_{Co\text{-}N}(\alpha_N'^2 + \alpha_N'''^2) \qquad (16b)$$

suffer from the drawback that the precise orientation of principal *A* values is not known. In view of the need for the use of appropriate symmetry models, such comparisons should await a single-crystal study of comparable O_2 and NO adducts. Nevertheless, one should remain a little cautious in view of the molecular-orbital calculations already mentioned where electron transfer appears to involve the ligand as well as the cobalt atom.

If it were possible to follow the method of the previous paragraph, then the extent of electron transfer (e.t.) from metal to oxygen in the bond region would be that given by equation (17). At the moment, electron transfer

$$\text{e.t.} = 2(1 - \alpha'^2 - \alpha'''^2) - 1 \qquad (17)$$

cannot be calculated reliably. While the specific details of the theory advanced by Tovrog *et al.* need to be changed, it must also be pointed out that Drago[18] has indicated some of the qualifications embodied in that work.

g Values. The *g* values originally calculated by Kanzig and Cohen,[26] for O_2^- in KCl crystals, have often been referred to in connection with Co–O_2 adducts. They are based upon a removal of degeneracy between the $\pi^*(x_g)$ and $\pi^*(z_g)$ orbitals upon formation of O_2^-. For g_x and g_z (Figure 4), first-order corrections were also given arising from spin–orbit coupling to a filled $2p\sigma_g$ low-lying state. In theory, g_x and g_z remain very close to 2 while g_y, along the O–O bond, is given by equation

$$g_y = 2 + 2[\lambda^2/(\lambda^2 + \Delta^2)]^{\frac{1}{2}} \qquad (18)$$

(18) where λ is the oxygen spin–orbit coupling and Δ the energy separation between $\pi^*(x_g)$ and $\pi^*(2_g)$. For O_2^-

TABLE 11

Elemental analyses of the metal chelates of salicylaldazinate (salaz), 5,5′-dichlorosalicylaldazinate (dcsalaz), and 3,3′-dimethoxysalicylaldazinate (dmsalaz)

	Found (%)			Calculated (%)			
Compound	C	H	N	C	H	N	$\mu_{eff.}$/B.M. *
[Co(salaz)]·2H_2O	50.75	4.20	8.50	50.45	4.20	8.40	4.34
[Ni(salaz)]·2H_2O	50.65	4.25	8.40	50.65	4.20	8.45	3.28
[Cu(salaz)]·2H_2O	50.0	4.15	8.30	49.8	4.15	8.30	1.85
[Mn(salaz)]·2H_2O	51.0	4.20	8.60	51.1	4.25	8.50	5.81
[Co(dcsalaz)]·2H_2O	41.9	3.40	6.90	41.8	3.50	6.95	4.52
[Ni(dcsalaz)]·2H_2O	41.85	3.45	6.90	41.8	3.45	6.95	3.36
[Cu(dcsalaz)]·2H_2O	41.25	3.45	6.90	41.3	3.45	6.90	1.91
[Mn(dcsalaz)]·2H_2O	42.2	3.50	7.10	42.2	3.50	7.05	5.89
[Co(dmsalaz)]·2H_2O	45.4	4.80	7.55	45.55	4.90	7.60	4.30
[Ni(dmsalaz)]·2H_2O	45.65	4.85	7.80	45.6	4.80	7.65	3.34
[Cu(dmsalaz)]·2H_2O	45.05	4.80	7.60	44.95	4.80	7.50	1.83
[Mn(dmsalaz)]·2H_2O	46.0	4.90	7.70	46.05	4.95	7.65	5.84

* 1 B.M. = 9.274×10^{-24} A m^2.

in potassium chloride crystals, the two oxygens are equivalent, whereas in almost all of the Co–O_2 adducts so far reported the oxygens are inequivalent. Furthermore, in view of the fact that to explain cobalt h.f.s. one may need to alter the cobalt *d*-orbital energies of Figure 7, it is possible that the oxygen molecular-orbital scheme used to obtain the *g* values by Kanzig and Cohen may need some reassessment.

TABLE 12

Weight losses for the transition-metal chelates of salicylaldazine with increase in temperature

Chelate	Weight loss (%)	θ_c/°C
$[Co^{II}(salaz)]\cdot 2H_2O$	5.2	75
	10.2	162
$[Cu^{II}(salaz)]\cdot 2H_2O$	5.4	76
	10.8	163
$[Mn^{II}(salaz)]\cdot 2H_2O$	5.3	73
	10.1	165
$[VO(salaz)]\cdot 2H_2O$	5.9	73
	11.2	164
$[Ni^{II}(salaz)]\cdot 2H_2O$	5.2	75
	10.8	165
$[Fe^{II}(salaz)]\cdot 2H_2O$	5.1	74
	10.4	164

TABLE 13

Analytical and magnetic susceptibility data for the metal chelates of the salicylaldehyde hydrazone anion (salhy)

Chelate	Calculated (%)			Found (%)			$\mu_{eff.}$/B.M. *
	C	H	N	C	H	N	
$[Cu^{II}(salhy)_2(OH_2)_2]$	44.4	4.65	15.05	44.35	4.65	14.85	1.89
$[Co^{II}(salhy)_2(OH_2)_2]$	45.9	4.85	15.05	45.8	4.80	15.0	4.91
$[Ni^{II}(salhy)_2(OH_2)_2]$	46.25	4.95	15.65	46.25	5.05	15.7	2.97
$[Mn^{II}(salhy)_2(OH_2)_2]$	46.25	5.00	15.2	46.25	5.10	15.1	6.03
$[Fe^{II}(salhy)_2(OH_2)_2]$	46.15	4.85	15.5	46.2	4.75	15.6	5.03
$Cu^{II}Cl_2\cdot 4salhy$	49.2	4.80	16.5	49.2	4.80	16.7	1.88
$Co^{II}Cl_2\cdot 4salhy$	49.85	4.55	16.6	49.9	4.60	16.5	4.83
$Ni^{II}Cl_2\cdot 4salhy$	49.85	4.75	16.65	49.95	4.80	16.65	3.20
$Fe^{II}(SO_4)\cdot 4salhy$	48.3	4.60	16.7	48.3	4.70	16.9	4.93
$MnCl_2\cdot 4salhy$	50.15	4.80	16.7	50.25	4.80	16.95	6.08

* 1 B.M = 9.274×10^{-24} A m^2.

EXPERIMENTAL

Absorption spectra in the u.v.–visible region were recorded on a Unicam SP 800 spectrophotometer at room temperature using 1-cm pathlength glass cells. The i.r. spectra were obtained on a Jasco IRA-1 diffraction grating spectrophotometer using sodium chloride plates. The e.s.r. spectra were recorded using a Varian E-12 spectrometer employing 100 kHz modulation. All e.s.r. measurements were carried out at about 9 149 Hz. Cooling of the sample was provided by a nitrogen flow system. Magnetic susceptibility measurements were made at room temperature by the Gouy method using glass sample tubes and corrected for diamagnetism.

Salicylaldazine was prepared as outlined [27] by treating salicylaldehyde (8.5 g) in ethanol (50 cm^3) with hydrazine hydrate (1.8 g) dissolved in ethanol (25 cm^3). The mixture was stirred for 5 min when the product separated, followed by recrystallization from hot ethanol. The other salicylaldazine derivatives were prepared in a similar manner using the appropriate aldehyde. Salicylaldehyde hydrazone was prepared by a modification of the method outlined by Jain and Kamar.[27] Salicylaldehyde (12.2 g) was added to hydrazine hydrate (5.0 g) dissolved in ethanol (50 cm^3). Ice-cold water (50 cm^3) was added to the reaction mixture with constant stirring. The white product formed was filtered off, washed with ice-cold water, and recrystallized from ethanol. All the other salicylaldehyde derivatives were prepared in a similar way using the appropriate aldehyde.

Preparation of the Cobalt(II) *Chelate of Salicylaldazine.*—To a solution of salicylaldazine (2.40 g) in dimethylformamide (50 cm^3) was added an aqueous solution (50 cm^3) of hydrated cobalt(II) chloride (2.5 g) followed by triethylamine (2.2 g). The product was isolated by addition of an excess (100 cm^3) of ice-cold water. The chelate was filtered off, recrystallized from water–ethanol (1 : 4), and air dried.

The elemental analyses and magnetic susceptibility data for the cobalt(II) chelates of salicylaldazine, 5,5′-dichlorosalicylaldazine, and 3,3′-dimethoxysalicylaldazine as well as those of the chelates of nickel(II), copper(II), and manganese(II) prepared in a similar manner are shown in Table 11. The gravimetric data showing the loss of water by the chelates with progressive rises in temperature are summarized in Table 12.

Preparation of the Cobalt(II) *Chelate of Salicylaldehyde Hydrazone.*—The cobalt(II) chelates as well as those of copper(II), nickel(II), manganese(II), and iron(II) were prepared by the method of Hunter and Marriot.[28] The elemental analyses and magnetic susceptibility data are summarized in Table 13.

This work was supported in part by the Australian Research Grants Committee. One of us (I. M. R.) acknowledges receipt of a Commonwealth Postgraduate Research Award.

[1/520 *Received*, 1*st April*, 1981]

REFERENCES

[1] R. J. Lancashire, T. D. Smith, and J. R. Pilbrow, *J. Chem. Soc., Dalton Trans.*, 1979, 66.

[2] M. Cajai, *Chem. Ber.*, 1898, **31**, 2807.

[3] C. S. Marvel and P. V. Bonsignore, *J. Am. Chem. Soc.*, 1959, **81**, 2668.

[4] S. Satapathy and B. Sahro, *J. Inorg. Nucl. Chem.*, 1970, **32**, 2223.

[5] R. G. R. Bacon and W. S. Lindsay, *J. Chem. Soc.*, 1958, 1382.

[6] W. J. Strattan and D. H. Busch, *J. Am. Chem. Soc.*, 1960, **82**, 4834.

[7] R. L. Ray, K. B. Pandeya, and R. P. Singh, *Indian J. Chem.*, 1974, **12**, 532.

[8] R. L. Ray, B. S. Garg, and R. P. Singh, *J. Chin. Chem. Soc. (Taipei)*, 1976, **23**, 47.

[9] R. C. Aggarwal, N. K. Singh, and R. P. Singh, *Inorg. Chim. Acta*, 1979, **32**, L87.

[10] F. A. Walker, *J. Magn. Reson.*, 1974, **15**, 201.

[11] J. A. de Bolfo, T. D. Smith, J. F. Boas, and J. R. Pilbrow, *J. Chem. Soc., Dalton Trans.*, 1976, 1495.

[12] J. R. Pilbrow and M. E. Winfield, *Mol. Phys.*, 1973, **25**, 1073.

[13] J. R. Pilbrow, *Mol. Phys.*, 1969, **16**, 307.

[14] R. Aasa and T. Vänngård, *J. Magn. Reson.*, 1975, **19**, 308.

[15] R. H. Niswander and L. T. Taylor, *J. Magn. Reson.*, 1977, **26**, 491.

[16] B. S. Tovrog, D. J. Kitko, and R. S. Drago, *J. Am. Chem. Soc.*, 1976, **98**, 5144.

[17] R. S. Drago, T. Beugelsdijk, J. A. Breese, and J. P. Cannady, *J. Am. Chem. Soc.*, 1978, **100**, 5374.

[18] R. S. Drago in 'ESR and NMR of Paramagnetic Species in Biological and Related Systems,' eds. I. Bertini and R. S. Drago, D. Reidel Publishing Co., Dordrecht, Holland, 1980, p. 51.

[19] L. C. Dickinson and J. C. W. Chien, *Proc. Natl. Acad. Sci. USA*, 1980, **17**, 1235.

[20] B. M. Hoffman, D. L. Diemente, and F. Basolo, *J. Am. Chem. Soc.*, 1970, **92**, 61.

[21] B. B. Wayland, J. V. Minkiewicz, and M. E. Abd-Elmageed, *J. Am. Chem. Soc.*, 1974, **96**, 2975.

[22] R. D. Harcourt, *Int. J. Quantum Chem.*, 1977, **4**, 143.

[23] A. Diedieu, M.-M. Rohmer, and A. Veillard, *J. Am. Chem. Soc.*, 1976, **98**, 5789.

[24] P. Fantucci and V. Valenti, *J. Am. Chem. Soc.*, 1976, **98**, 3832.

[25] G. A. Rodley and W. T. Robinson, *Nature (London)*, 1972, **235**, 438.

[26] W. Kanzig and M. H. Cohen, *Phys. Rev. Lett.*, 1959, **3**, 509.

[27] M. P. Jain and S. Kamar, *Talanta*, 1977, **24**, 149.

[28] L. Hunter and J. A. Marriot, *J. Chem. Soc.*, 1937, 2000.